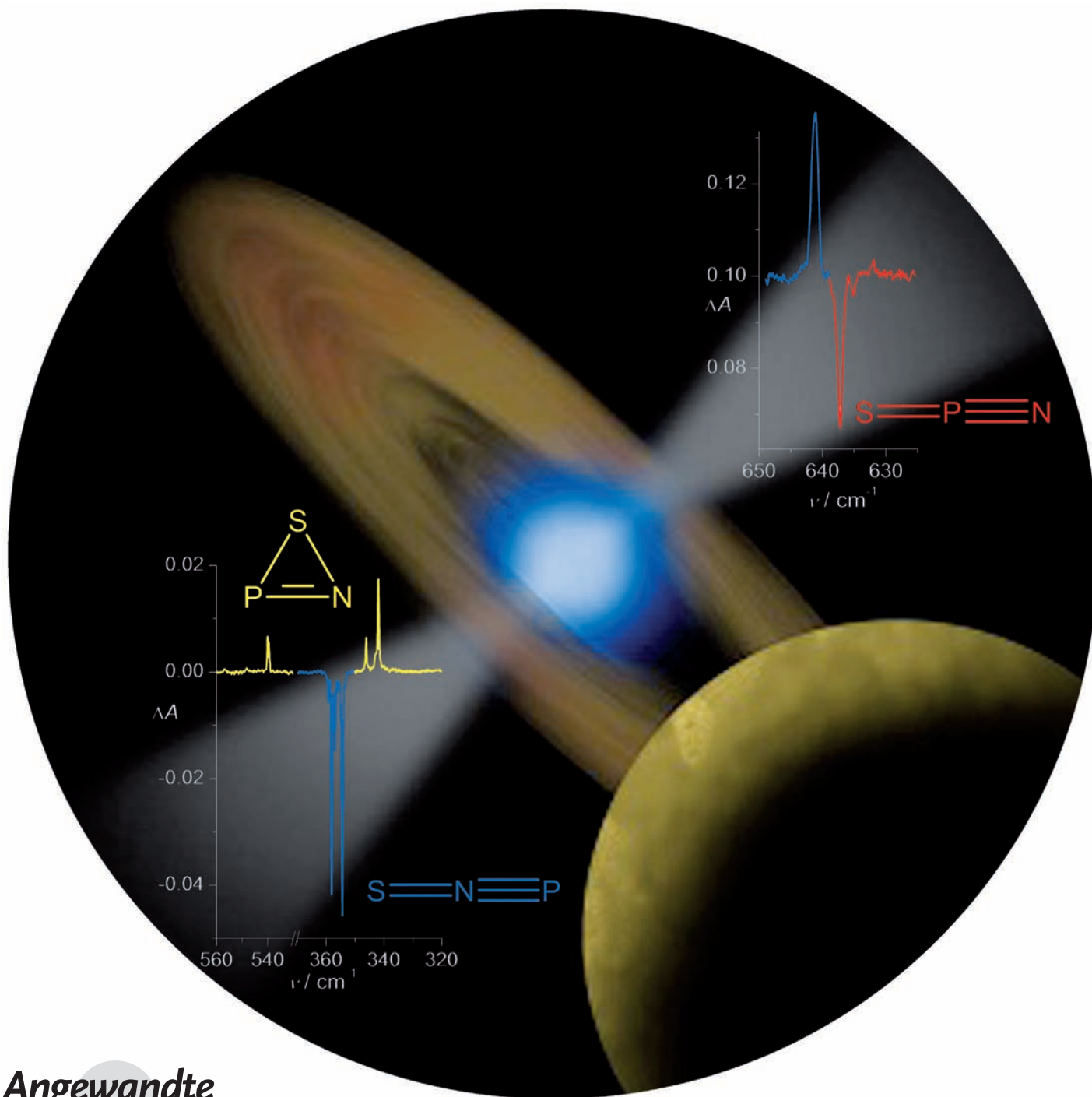**Small-Ring Systems**

Experimental Observation of the 16-Electron Molecules SPN, SNP, and Cyclic PSN**

Xiaoqing Zeng, Helmut Beckers, Helge Willner, and Joseph S. Francisco*

Dedicated to Professor Dianxun Wang on the occasion of his 70th birthday

Small molecules of second-row elements and their third-row analogues have been the focus of extensive theoretical and experimental studies due to their novel structure and bonding properties.[1] In particular, low-coordinated phosphorus molecules have been discovered in circumstellar and dense interstellar clouds,[2] and some phosphorus–nitrogen triply bonded species have been attracting much attention due to their applications as building blocks in organophosphorus chemistry.[3] The recent direct observation of diatomic PN in supergiant star VY CMa[4] suggests the existence of more phosphorus molecules in the presence of oxygen or sulfur. Moreover, elusive species such as N_2S,[5,6] P_2O/P_2S,[7,8] and OPN/SPN[9,10] have been of great interest. Dinitrogen sulfide (N_2S), first produced by the thermolysis of thiatriazoles, was confirmed to be a linear molecule with sulfur at the terminal position.[5,6] The diphosphorus compounds P_2O[7] and P_2S[8] have first been identified in solid argon matrices by its P=O stretching vibration (1270.4 cm^{-1}) and the isotope pattern of the P=S mode (^{32}S: 891.4 cm^{-1}, ^{34}S: 887.8 cm^{-1}), respectively. Both adopt a linear structure featuring a terminal P≡P bond. To date, cyclic isomers of P_2O and P_2S have not been detected.

After more than two decades since the discovery of ONP,[9] the OPN isomer was obtained by photolytic decomposition of $OP(N_3)_3$ in a solid Ar matrix.[10] However, their cyclic isomer was not found. As a rule, second-row triatomic molecules having 16 valence electrons adopt a linear structure.[11] This is because of the favorable involvement of these atoms in strong π-type bonds, and due to their unfavorable bonding in small rings.[12] Thus, their cyclic isomers, if they exist at all, are weakly bonded high-energy species.[13–15] On the other side, for the third and higher row analogues, which avoid using their s valence electrons in multiple bonding, cyclic molecules may become experimentally observable species.[13,14,16] However, to the best of our knowledge, cyclic third-row triatomic molecules having 16 valence electrons have not been observed so far.

Here, we report the first neutral cyclic third-row triatomic species, *cyc*-PSN, and its photointerconversion with two linear isomers SNP and SPN in solid noble gas matrices.

Preliminary exploration of the potential energy surface for the SPN system by using density functional calculations with the B3LYP/6-311+G(3df) method combined with intrinsic reaction coordinate (IRC) analysis shows that the linear SNP isomer is the global minimum. The barrier from

SPN to *cyc*-PSN is 138 kJ mol^{-1}, and *cyc*-PSN is separated from SNP by a barrier of 95 kJ mol^{-1}. CCSD(T)/cc-pVTZ calculations were consistent with the B3LYP results, and *cyc*-PSN and SPN are 93 and 73 kJ mol^{-1} higher in energy than SNP, respectively. The results, given in Figure 1, are consistent with previous calculations at the configuration interaction (CI) level.[13] The collective calculations and barriers suggest that all three isomers should be experimentally detectable at low temperatures.
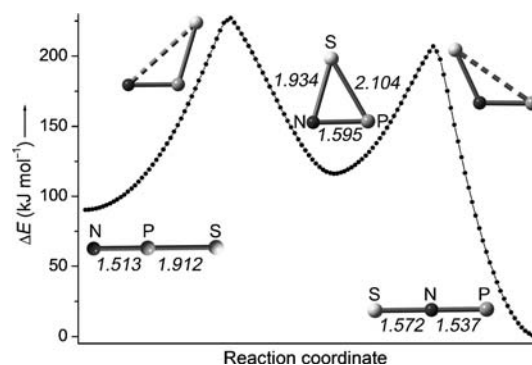

Figure 1. Calculated reaction coordinate of SPN isomers along the P-N-S angle at the B3LYP/6-311+G(3df) level of theory. Bond lengths [Å] of the minima calculated at the CCSD(T)/cc-pVTZ are given in italics.

The SPN molecule was generated experimentally by thermal or photolytic decomposition of $SP(N_3)_3$, which extrudes four moles of nitrogen molecules [Eq. (1)]. The highly explosive triazide precursor has been very recently obtained as a neat substance.[17]

$$SP(N_3)_3 \rightarrow SPN + 4N_2 \tag{1}$$

The triazide, diluted in Ar (approximately 1:1000) was heated to about 1000°C, and the mixture was then deposited onto the cold matrix support at 16 K. The IR spectrum (Figure S1 in the Supporting Information) shows that only traces of triazide were left. Among the products, the nitrogen-containing species of PN (1327.4 cm^{-1}, $\Delta\nu(^{14/15}N) = 30.3$ cm^{-1}),[18] SN (1208.6 cm^{-1}, $\Delta\nu(^{14/15}N) = 28.0$ cm^{-1}),[19] SN_2 (2039.9 cm^{-1}, $\Delta\nu(^{14/15}N) = 36.2$ cm^{-1}),[20] and HN_3 (2135.3 cm^{-1}, 1146.1 cm^{-1})[21] were identified by using ^{15}N labeling and by comparing to reference spectra. Traces of HN_3 might be formed from the hydrolysis of the triazide. Diatomic PS was also formed, as evidenced by the occurrence of a very weak band at 729.3 cm^{-1}, consistent with the reported value of 729.5 cm^{-1} in Ar matrix.[8]

Among the unknown IR bands, the strongest one at 1374.1 cm^{-1} was found to be accompanied by two weak bands at 641.2 cm^{-1} and 358.1/354.4 cm^{-1} (exhibiting matrix site splitting). Their band positions and relative intensities (Table 1) are in good agreement with the prediction for SNP at 1407, 661, and 358 cm^{-1} from the CCSD(T)/aug-cc-pV5Z level of theory. Their assignment to SNP is further supported by the isotopic shifts of the naturally abundant ^{34}S and the ^{15}N labeled samples summarized in Table 1. Accord-

[*] Dr. X. Q. Zeng, Dr. H. Beckers, Prof. Dr. H. Willner
Bergische Universität Wuppertal, FB C, Mathematik und Naturwissenschaften, Fachgruppe Chemie
Gaußstr. 20, 42119 Wuppertal (Germany)
E-mail: zeng@uni-wuppertal.de

Prof. Dr. J. S. Francisco
Purdue University, Department of Chemistry
West Lafayette, IN 47907-2084 (USA)
E-mail: francisc@purdue.edu

Supporting information for this article is available on the WWW under http://dx.doi.org/10.1002/anie.201108636.

Table 1: Observed and calculated IR frequencies [cm^{-1}] of SPN isomers.

Species	Mode number	Mode description	Observed[a] Ar matrix	CCSD(T) cc-pVTZ[c]	aug-cc-pVQZ	aug-cc-pV5Z	^{15}N[b] obsd	calcd[d]	^{34}S[b] obsd	calcd[d]
SNP	1	PN stretch	1374.1 (100)	1403 (384)	1401	1407	33.0	38.4	2.5	2.4
	2	NS stretch	641.2 (1)	652 (4)	657	661	2.1	0.2	9.2	10.2
	3	SNP bend	358.1/354.4 (4)	353 (11)	353	358	9.8	9.7	0.8	0.9
cyc-PSN	1	PN stretch		1049 (1)	1062	1069		24.0		
	2	Sym-ring	540.0 (34)	543 (2)	548	552	4.2	4.1		
	3	Asym-ring	346.1/341.9 (100)	330 (27)	345	351	5.9	5.9		
SPN	1	PN stretch	1314.4 (55)	1313 (0.5)	1321	1331	24.0	28.0		
	2	PS stretch	637.1 (100)	630 (33)	639	644	4.9	4.7		
	3	SPN bend	196.8/195.2 (24)	191 (5)	193	194	2.3	2.6		

[a] Observed band positions in Ar matrix and relative integrated intensities in parenthesis. [b] Isotopic shifts relative to the natural ^{14}N and ^{32}S sample. [c] The IR intensities [km mol^{-1}] in parentheses were calculated at the MP2/cc-pVTZ level of theory based on the CCSD(T)/cc-pVTZ optimized structures. [d] Calculations at the CCSD(T)/cc-pVTZ level of theory.

ing to the very different ^{15}N isotopic shifts of the two stretching vibrations of ν_1 (33.0 cm^{-1}) and ν_2 (2.1 cm^{-1}), they are more appropriately described as out-of-phase and in-phase S-N-P stretches, respectively. Due to a Fermi resonance, the first band of S^{15}NP splits into two bands at 1341.4 (ν_1) and 1329.1 cm^{-1} ($\nu_2 + 2\nu_3$), in which the sum of their intensities is almost equal to that of S^{14}NP (Figure S2). No indication for the presence of the less stable isomers was obtained in the pyrolysis of the triazide at about 1000 °C. Thus, SNP seems to be the most robust isomer against further decomposition.

When UV irradiation ($\lambda = 255$ nm, 20 min) was applied to the matrix-isolated pyrolysis products of the triazide, the IR spectrum clearly showed the selective depletion of the bands associated with SNP. Two weak bands at 1314.4 and 637.1 cm^{-1} in the mid-infrared region (MIR, Figure 2a), and three even weaker ones at 540.0, 346.1/341.9, and 196.8/195.2 cm^{-1} in the far-infrared region (FIR, Figure 3a), appeared simultaneously. The two new bands in the MIR are assigned to the SPN isomer, which was calculated to have three weak IR absorptions at 1331, 644, and 194 cm^{-1} at the
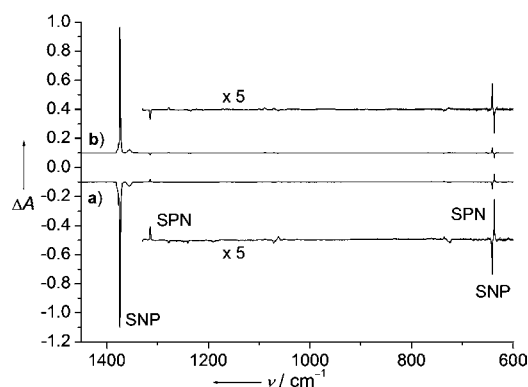

Figure 3. IR spectral changes in the region of 560–190 cm^{-1} obtained a) after UV light irradiation ($\lambda = 255$ nm), b) subsequent UV/vis irradiation ($\lambda > 395$ nm), and c) further UV/vis irradiation ($\lambda > 280$ nm) of an Ar matrix which contains the pyrolysis products of SP(N$_3$)$_3$. IR bands are assigned to either SPN, SNP, or *cyc*-PSN, and the bands of depleted species point downward and those of formed species upward. The feature marked by an asterisk is an artificial spike caused by the spectrometer.

Figure 2. IR spectral changes in the region of 1450–600 cm^{-1} obtained a) after UV light irradiation ($\lambda = 255$ nm), and b) subsequent UV irradiation ($\lambda = 330$ nm) of an Ar matrix which contains the pyrolysis products of SP(N$_3$)$_3$. IR bands are assigned to either SPN or SNP, and the bands of depleted species point downward and those of formed species upward.
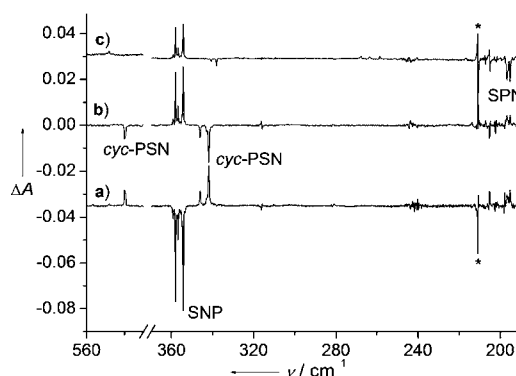
CCSD(T)/aug-cc-pV5Z level of theory (Table 1). The observed rather weak band at 196.8/195.2 cm^{-1} in the FIR is reasonably assigned to the bending mode of SPN. This assignment is supported by the $^{14/15}$N isotope shifts in Table 1, which agree quite well with the predictions. A $^{32/34}$S isotopic shift of 10.8 cm^{-1} for the strongest band (637.1 cm^{-1}) was also observed, which is in line with the prediction of 10.9 cm^{-1}.

The observed band positions for the remaining two weak bands in the FIR at 540.0 and 346.1/341.9 cm^{-1} are very close to the CCSD(T)/aug-cc-pV5Z predicted frequencies for the *cyc*-PSN isomer at 552 and 351 cm^{-1}, for the in-phase and out-of-phase P-S-N stretches, respectively. This assignment is corroborated by their $^{14/15}$N isotope shifts (Table 1). Features due to the naturally abundant *cyc*-P^{34}SN were not observed. Due to the low abundance of *cyc*-PSN in the matrix and also the low IR intensity, the P−N stretch was not observed in our experiments. The lack of intensity for the breathing mode makes such cyclic triatomic molecules generally difficult to observe in the MIR region, especially for third and higher row

analogues, for which the stronger out-of-phase stretches are expected to appear in the FIR region.[14] This probably explains why similar cyclic species have not yet been experimentally detected. The *cyc*-PSN isomer represents the first observed 16-electron cyclic third-row triatomic molecule. Another experimentally known cyclic third-row triatomic molecule is SiC$_2$ (12-electron).[22]

In subsequent experiments, visible light irradiation ($\lambda >$ 395 nm, 20 min) was applied to the matrix, this resulted in the conversion of *cyc*-PSN to SNP (Figure 3b) and also traces of SPN. Further UV/vis irradiation ($\lambda >$ 280 nm) caused isomerization from SPN to SNP (Figure 3c). Such conversion was also accomplished by a more selective UV irradiation of $\lambda = 330$ nm (Figure 2b). A similar photolytic interconversion was observed for the two linear PNO and NPO isomers.[10]

In addition to the thermal decomposition of SP(N$_3$)$_3$, its photolysis in solid Ar was studied. Notably, a stepwise dissociation of the triazide was observed. First, the azido nitrene ((N$_3$)$_2$P(S)N) was formed upon photolysis ($\lambda = 193$ nm) with an ArF excimer laser, which then undergoes Curtius rearrangement to form N$_3$P(S)N$_4$ under visible light irradiation ($\lambda >$ 420 nm). The N$_3$P(S)N$_4$ further decomposed into SNP using UV/vis irradiation of $\lambda >$ 320 nm (Figure S3). Since the IR bands associated with the two azide intermediates were found to be rather weak and complicated by matrix site splittings, their identification was mainly aided by DFT B3LYP/6-311 + G(3df) calculations (Figure S4 and Table S1). Based on the above observations, the thermal and photolytic decomposition pathways of SP(N$_3$)$_3$ are summarized in Scheme 1. In both cases, the final decomposition product is the most stable SNP isomer, which forms SPN and *cyc*-PSN isomers by selective irradiations.

The structural and bonding properties of the three SPN isomers were explored by using coupled-cluster calculations combined with natural bond orbital (NBO) analysis. A complete set of optimized structural parameters is given in Table 2 along with rotational constants for all isomers. For the two linear isomers, the bonding situations, elucidated in Scheme 2, are similar to the corresponding OPN isomers. The structural features of the SNP and SPN molecules can be explained by two Lewis resonance structures. A phosphorus–nitrogen triple bond in SPN is evidenced by a P—N stretching frequency of 1314.4 cm^{-1}, which is close to that of diatomic PN (1327.4 cm^{-1}). The calculated P—N bond lengths in SPN (1.502 Å) and SNP (1.527 Å) at the CCSD(T)/aug-cc-pV5Z level of theory are slightly larger than the sum of the triple bond covalent radii for P (0.94 Å) and N (0.54 Å).[23] Thus, SPN is regarded to be one of the very few examples[7,8,10] with phosphorus in a $\sigma^2\lambda^5$ coordination. For the cyclic isomer, the P—N bond length is calculated to be 1.582 Å, within the sum of the double bond covalent radii for P (1.02 Å) and N (0.60 Å).[23] The CCSD(T)/aug-cc-pV5Z calculated S—P and S—N bond lengths are 2.074 and 1.924 Å, respectively. The NBO analysis shows significant positive charge on P ($+1.02e$) and negative charge on N ($-0.90e$). The calculated very long S—N bond and the small negative charge on S ($-0.11e$)
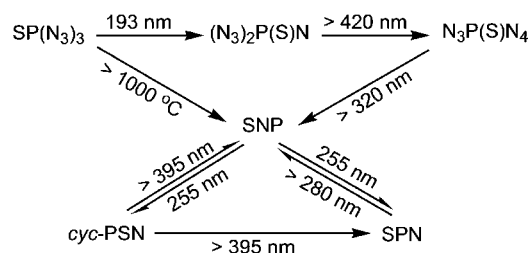

Scheme 1. Formation of SPN isomers.

Table 2: Molecular structure and rotational constants for SPN isomers.

Species, ABC	Basis set	Structure[a]			Rotational constants[b]		
		R(AB)	R(BC)	θ(ABC)	A	B	C
SNP	cc-pVTZ	1.573	1.537	180.0		3321	3321
	aug-cc-pVTZ	1.575	1.538	180.0		3314	3314
	aug-cc-pVQZ	1.567	1.503	180.0		3348	3348
	aug-cc-pV5Z	1.563	1.527	180.0		3365	3365
cyc-PSN	cc-pVTZ	2.104	1.934	46.3	23043	7098	5427
	aug-cc-pVTZ	2.103	1.938	46.3	22950	7109	5428
	aug-cc-pVQZ	2.084	1.930	46.4	23122	7232	5509
	aug-cc-pV5Z	2.074	1.924	46.4	23224	7294	5550
SPN	cc-pVTZ	1.912	1.513	180.0		3937	3937
	aug-cc-pVTZ	1.914	1.514	180.0		3933	3933
	aug-cc-pVQZ	1.902	1.506	180.0		3983	3983
	aug-cc-pV5Z	1.895	1.502	180.0		4009	4009

[a] Bond lengths in Å and angles in °, respectively. [b] In units of MHz.
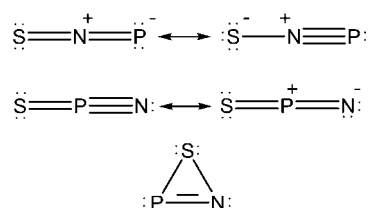
Scheme 2. Bonding properties of three SPN isomers.

suggest that this cyclic isomer is very flexible, and may easily undergo ring-opening or eliminate sulfur at high temperatures. This probably prevents its observation under the flash pyrolysis conditions. Indeed, the formation of PN[24] and S$_2$[25] fragments by the flash vacuum pyrolysis (FVP) of SP(N$_3$)$_3$ has been confirmed by their characteristic UV spectra (Figures S5 and S6).

Frontier molecular orbitals (FMOs) for the three SPN isomers were also examined. Their highest occupied (HOMOs) and lowest unoccupied molecular orbitals (LUMOs) are depicted in Figure 4. The FMOs of the two linear isomers are similar to those of the corresponding PNO isomers.[26] Replacement of O by S alters the HOMOs by a large contribution from the sulfur p orbital. For the cyclic isomer, the HOMO is a combination of the out-of-plane P—N bonding π-orbital with nonbonding to the sulfur p orbital, and the LUMO is simply the π*(P—N) orbital.
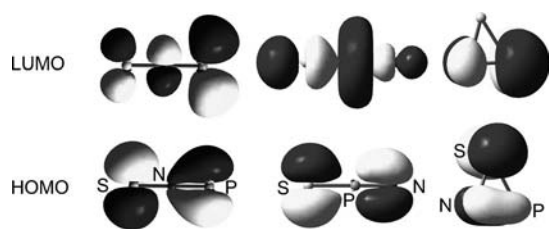
Figure 4. Molecular orbital plots (isovalue = 0.04) of the HOMO and LUMO for SNP, SPN, and *cyc*-PSN at the CCSD(T)/cc-pVTZ level of theory.

Experimental Section

Caution! Covalent azides are hazardous and explosive, and hence $SP(N_3)_3$ should be handled in submillimolar quantities only. Although we have not experienced any explosions during this work, safety precautions of wearing face shields, leather gloves, and protective leather clothes are strongly recommended when handling liquid and solid $SP(N_3)_3$.

Thiophosphoryl triazide, $SP(N_3)_3$, was prepared and purified according to published protocols.[17] 1-^{15}N sodium azide (98 atom% ^{15}N, EURISO-TOP GmbH) was used for preparing the ^{15}N labeled sample.

Matrix IR spectra were recorded on a FT-IR spectrometer (IFS 66v/S Bruker) in a reflectance mode using a transfer optic. A KBr beam splitter and MCT detector were used in the region of 4000–500 cm^{-1} and a Ge-coated 6-μ Mylar beam splitter with a He(l) cooled Si bolometer in the region of 700–180 cm^{-1} (CsI window). For each spectrum, 200 scans at a resolution of 0.25 cm^{-1} were co-added. Matrix UV/vis spectra were measured with the PerkinElmer Lambda 900 UV spectrometer in the range of 200 to 700 nm with a data point distance of 0.5 nm and an integration time of 2 s. The radiation of the spectrometer was directed into a 150 cm long optical quartz fiber, through a quartz lens inside the cryostat and twice passed through the matrix deposit on the cold Rh mirror. A second quartz lens and fiber collected the reflected radiation and returned it to the spectrometer. Details of the matrix apparatus have been described elsewhere.[27]

The gaseous sample was mixed by passing a flow of argon gas through a U-trap containing ca. 10 mg of solid $SP(N_3)_3$, which was kept in a cold ethanol bath at $-27°C$. By adjusting the flow rate of argon gas (2 mmol h^{-1}), a small amount of the resulting mixture (azide/Ar ≈ 1:1000 estimated) was deposited at a high vacuum within 30 min onto the matrix support (16 K for Ar matrix, 6 K for Ne matrix, Rh-plated Cu block), and used for photolysis experiments. For the pyrolysis experiments, the gas mixture was passed through an aluminium oxide tube furnace (i.d. 1.0 mm, o.d. 2.8 mm, length 25 mm), which was heated (voltage 5.3 V, current 2.0 A) to about 1000°C over a length of ca. 10 mm with a tantalum wire (o.d. 0.25 mm, resistance 0.8 Ω), prior to deposition on the cold matrix support in high vacuum.

Photolysis experiments were carried out with an ArF excimer laser (Lambda-Physik, 193 nm, 5 Hz), or with a high-pressure mercury arc lamp (TQ 150, Heraeus) by conducting the light through water-cooled quartz lenses combined with different Schott cut off filters of ≥ 280, ≥ 360, ≥ 395, ≥ 420, ≥ 455, and ≥ 570 nm, or Schott interference filter of 255 nm (Schott) and band-pass filter of 330FS10–50 (Lot-Oriel).

Computational details: The structures and IR frequencies were calculated using coupled cluster theory with single and double excitation, and including a perturbative triples correction (CCSD(T)) method[28] and the following basis sets: cc-pVTZ, augmented aug-cc-pVQZ and aug-cc-pV5Z.[29] Their IR intensities were estimated at the CCSD(T)/cc-pVTZ optimized structures using the second-order Møller-Plesset (MP2) approximation at the same basis set.[30] Local minima were confirmed by vibrational frequency analysis, and transition states were confirmed by intrinsic reaction coordinate (IRC) calculations.[31] Natural bond order (NBO) analysis was performed using NBO 3.1 implemented in Gaussian 03 with the B3LYP method.[32] All calculations were performed using the Gaussian 03 software package.[33]

[1] See, for recent examples: a) V. Lattanzi, S. Thorwirth, D. T. Halfen, L. A. Mück, L. M. Ziurys, P. Thaddeus, J. Gauss, M. C. McCarthy, *Angew. Chem.* **2010**, *122*, 5795–5798; *Angew. Chem. Int. Ed.* **2010**, *49*, 5661–5664; b) S. Thorwirth, L. A. Mück, J. Gauss, F. Tamassia, V. Lattanzi, M. C. McCarthy, *J. Phys. Chem. Lett.* **2011**, *2*, 1228–1231; c) X. Q. Zeng, H. Beckers, H. Willner, J. F. Stanton, *Angew. Chem.* **2011**, *123*, 1758–1761; *Angew. Chem. Int. Ed.* **2011**, *50*, 1720–1723; d) R. Evans, A. J. Downs, R. Köppe, S. C. Peake, *J. Phys. Chem. A* **2011**, *115*, 5127–5137; e) E. G. Hohenstein, H. M. Jaeger, E. J. Carrell, G. S. Tschumper, C. D. Sherrill, *J. Chem. Theory Comput.* **2011**, *7*, 2842–2851; f) F. X. Sunahori, J. Wei, D. J. Clouthier, *J. Am. Chem. Soc.* **2007**, *129*, 9600–9621.

[2] L. M. Ziurys, *Proc. Natl. Acad. Sci. USA* **2006**, *103*, 12274–12279.

[3] See for examples: a) R. Kinjo, B. Donnadieu, G. Bertrand, *Angew. Chem.* **2010**, *122*, 6066–6069; *Angew. Chem. Int. Ed.* **2010**, *49*, 5930–5933; b) G. Sicard, A. Baceiredo, G. Bertrand, J. P. Majoral, *Angew. Chem.* **1984**, *96*, 450–451; *Angew. Chem. Int. Ed. Engl.* **1984**, *23*, 459–460; c) A. Baceiredo, G. Bertrand, J.-P. Majoral, G. Sicard, J. Jaud, J. Galy, *J. Am. Chem. Soc.* **1984**, *106*, 6088–6089; d) R. Appel in *Multiple Bonds and Low Coordination in Phosphorus Chemistry* (Eds.: M. Regitz, O. J. Scherer), Thieme, Stuttgart, **1990**, pp. 157–219.

[4] L. M. Ziurys, S. N. Milam, A. J. Apponi, N. J. Woolf, *Nature* **2007**, *447*, 1094–1097.

[5] C. Wentrup, P. Kambouris, *Chem. Rev.* **1991**, *91*, 363–373, and references therein.

[6] a) R. D. Davy, H. F. Schaefer III, *J. Am. Chem. Soc.* **1991**, *113*, 1917–1922; b) A. A. Bhattacharyya, A. Bhattacharyya, R. R. Adkins, A. G. Turner, *J. Am. Chem. Soc.* **1981**, *103*, 7458–7465; c) A. T. Wong, G. B. Bacskay, *Chem. Phys. Lett.* **1994**, *217*, 17–23.

[7] a) L. Andrews, R. Withnall, *J. Am. Chem. Soc.* **1988**, *110*, 5605–5611; b) I. S. Bell, H.-B. Qian, P. A. Hamilton, P. B. Davies, *J. Chem. Phys.* **1997**, *107*, 8311–8316; c) C. W. Bauschlicher, Jr., M. Zhou, L. Andrews, *J. Phys. Chem. A* **2000**, *104*, 3566–3571.

[8] Z. Mielke, G. D. Brabson, L. Andrews, *J. Phys. Chem.* **1991**, *95*, 75–79.

[9] R. Ahlrichs, S. Schunck, H. Schnöckel, *Angew. Chem.* **1988**, *100*, 418–420; *Angew. Chem. Int. Ed. Engl.* **1988**, *27*, 421–423.

[10] X. Q. Zeng, H. Beckers, H. Willner, *J. Am. Chem. Soc.* **2011**, *133*, 20696–20699.

[11] A. D. Walsh, *J. Chem. Soc.* **1953**, 2266–2288.

[12] Y. Naruse, S. Inagaki, *Top. Curr. Chem.* **2009**, *289*, 265–291.

[13] T. Busch, W. W. Schoeller, *Z. Phys. D* **1989**, *13*, 289–294.

[14] R. D. David, S. Holiday, *Chem. Phys. Lett.* **1995**, *232*, 313–318.

[15] D. Feller, J. Katriel, E. R. Davidson, *J. Chem. Phys.* **1980**, *73*, 4517–4520.

[16] Y.-H. Ding, K. Takeuchi, S. Inagaki, *Chem. Lett.* **2004**, *33*, 934–935.

[17] X. Q. Zeng, E. Bernhardt, H. Beckers, H. Willner, *Inorg. Chem.* **2011**, *50*, 11235–11241.

[18] R. M. Atkins, P. L. Timms, *Spectrochim. Acta Part A* **1977**, *33*, 853–857.

[19] P. Hassanzadeh, L. Andrews, *J. Am. Chem. Soc.* **1992**, *114*, 83–91.

[20] P. Kambouris, T. K. Ha, C. Wentrup, *J. Phys. Chem.* **1992**, *96*, 2065–2068.

[21] H.-J. Himmel, M. Junker, H. Schnöckel, *J. Chem. Phys.* **2002**, *117*, 3321–3326.

[22] G. Maier, H. Pacl, H. P. Reisenauer, A. Meudt, R. Janoschek, *J. Am. Chem. Soc.* **1995**, *117*, 12712–12720, and references therein.

[23] P. Pyykkö, S. Riedel, M. Patzschke, *Chem. Eur. J.* **2005**, *11*, 3511–3520.

[24] J. Curry, L. Herzberg, G. Herzberg, *Z. Phys.* **1933**, *86*, 348–366.

[25] L. Brewer, G. D. Brabson, B. Meyer, *J. Chem. Phys.* **1965**, *42*, 1385–1389.

[26] D. J. Grant, D. A. Dixon, A. E. Kemeny, J. S. Francisco, *J. Chem. Phys.* **2008**, *128*, 164305.

[27] H. G. Schnöckel, H. Willner in *Infrared and Raman Spectroscopy, Methods and Applications* (Ed.: B. Schrader), VCH, Weinheim, **1994**.

[28] a) G. D. Purvis III, R. J. Bartlett, *J. Chem. Phys.* **1982**, *76*, 1910–1918; b) K. Raghavachari, G. W. Trucks, J. A. Pople, M. Head-Gordon, *Chem. Phys. Lett.* **1989**, *157*, 479–483; c) J. D. Watts, J. Gauss, R. J. Bartlett, *J. Chem. Phys.* **1993**, *98*, 8718–8733.

[29] a) D. E. Woon, T. H. Dunning, *J. Chem. Phys.* **1993**, *98*, 1358–1371; b) T. H. Dunning, *J. Chem. Phys.* **1989**, *90*, 1007–1023; c) R. A. Kendall, T. H. Dunning, R. J. Harrison, *J. Chem. Phys.* **1992**, *96*, 6796–6806.

[30] C. Møller, M. S. Plesset, *Phys. Rev.* **1934**, *46*, 618–622.

[31] a) C. Gonzalez, H. B. Schlegel, *J. Chem. Phys.* **1989**, *90*, 2154–2161; b) C. Gonzalez, H. B. Schlegel, *J. Phys. Chem.* **1990**, *94*, 5523–5527.

[32] A. E. Reed, L. A. Curtiss, F. Weinhold, *Chem. Rev.* **1988**, *88*, 899–926.

[33] Gaussian 03 (Revision B.05): M. J. Frisch et al., see the Supporting Information.